BNL-204652-2018-JAAM

# Optimization methodology for the global 10 Hz orbit feedback in RHIC

C. Liu,

To be published in "Nuclear Instruments and Methods in Physics Research Section A: Accelerators, Spectrometers, Detectors and Associated Equipment"

May 2018

Collider Accelerator Department

**Brookhaven National Laboratory**

**U.S. Department of Energy**

USDOE Office of Science (SC), Nuclear Physics (NP) (SC-26)

# DISCLAIMER

# Optimization methodology for the global 10 Hz orbit feedback in RHIC

C. Liu, R. Hulsart, K. Mernick, R. Michnoff, M. Minty

*Brookhaven National Laboratory, Upton, NY, U.S.A.*

**Abstract**

To combat beam oscillations induced by triplet vibrations at the Relativistic Heavy Ion Collider (RHIC), a global orbit feedback system was developed and applied at injection and top energy in 2011, and during beam acceleration in 2012. Singular Value Decomposition (SVD) was employed to determine the strengths and currents of the applied corrections. The feedback algorithm was optimized for different magnetic configurations (lattices) at fixed beam energies and during beam acceleration. While the orbit feedback performed well since its inception, corrector current transients and feedback-induced beam oscillations were observed during the polarized proton program in 2015. In this report, we present the feedback algorithm, the optimization of the algorithm for various lattices and the solution adopted to mitigate the observed current transients during beam acceleration.

*Keywords:* orbit correction, orbit feedback, triplet vibration, singular value decomposition (SVD), eigenvalue, Tikhonov regularization

## 1. Introduction

RHIC (Fig. 1) comprises two circular counter-rotating superconducting accelerators in a common horizontal plane, which are oriented to intersect one another at six interaction points (IPs) with two colliding beam experiments (STAR and PHENIX) [1]. Each accelerator consists of three inner arcs and three outer arcs with six insertions joining them. A dipole magnet (DX magnet) on each side of each IP brings the beams together for head-on collisions for

*Email address:* cliu1@bnl.gov (C. Liu)

experiments. The DX magnets are the only common bending magnets for the two rings. The triplets (Q1, Q2 and Q3 quadrupole magnets) focus the beam to small beam sizes at the IPs. The triplets and D0 dipole magnets of both accelerators are installed in a common cryostat.

Fluctuations of the horizontal orbits with a frequency of about 10 Hz were observed during early RHIC commissioning in both rings [2]. Measurements using accelerometers mounted on the triplet magnets revealed dominant frequencies around 10 Hz [2]. Mechanical modeling of the triplet quadrupole supports also showed eigenfrequencies near 10 Hz [3, 4]. Oscillations in the Helium pressure around 10 Hz were measured and identified as the cause of triplet vibrations [3, 5]. The beam parameters and machine performance were affected by orbit variations [6]. Over the years several methods were considered to mitigate the orbit variations [7, 4].

A global orbit feedback system [8] was adopted and used successfully to mitigate the beam oscillations for many years. However, in 2015 due to a different lattice design, non-optimal performance, namely unexpected transients in the corrector response, was observed during beam acceleration. The feedback algorithm was then modified to mitigate the current transients. The algorithm used before 2015 and the necessitated changes will be reviewed in this article.

The orbit feedback algorithm will be presented in section 2. The numerical simulations and experimental confirmation of feedback optimization at fixed energies are presented in section 3, and during beam acceleration in section 4. The additional measures to mitigate corrector current transients observed in later years of operation will be presented in section 5. A summary will be given in section 6.

## 2. Orbit feedback algorithm

The algorithm is a least square fit to compensate the orbit oscillations using fast correctors [8, 9]. The corrector magnet currents $\theta$, needed to compensate the oscillations, are given by Eq. 1, where $< x >_i$ is the average position and

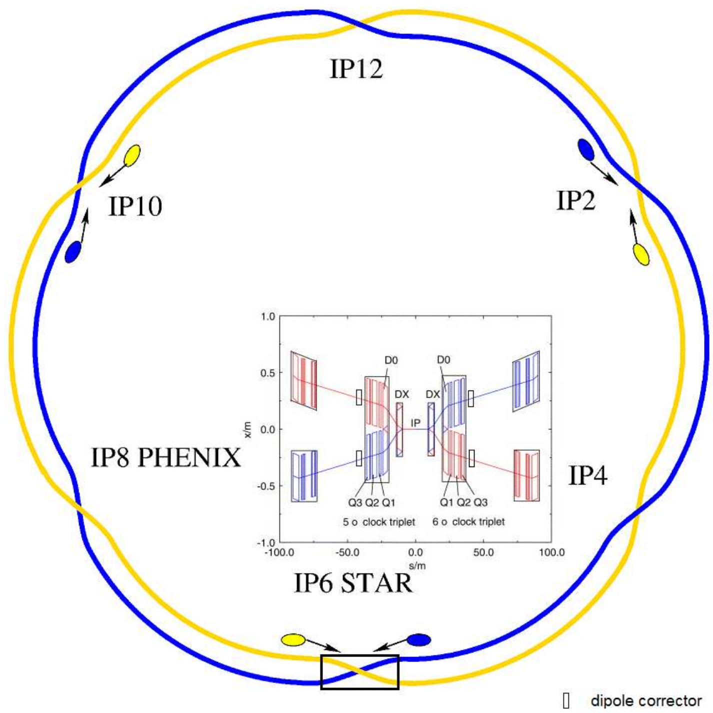


Figure 1: The schematic layout of RHIC with an expanded view of the STAR experimental area. The feedback system [8] in each accelerator consists of two BPMs in the triplet cryostat near the Q1 and Q3 magnets on each side of all six IPs, two BPMs in each arc and one dipole corrector at each triplet.

$x_i$ is the measured position at the $i$th BPM, the $m \times n$ matrix $R$ denotes the response of the beam positions to correctors, where $m$ represents the number of beam position monitors and $n$ the number of correctors,

$$\triangle X = \begin{pmatrix} <x>_1 - x_1 \\ <x>_2 - x_2 \\ \vdots \\ <x>_m - x_m \end{pmatrix} = \begin{pmatrix} R_{11} & R_{12} & \cdots & R_{1n} \\ R_{21} & R_{22} & \cdots & R_{2n} \\ \vdots & \vdots & \ddots & \vdots \\ R_{m1} & R_{m2} & \cdots & R_{mn} \end{pmatrix} \begin{pmatrix} \theta_1 \\ \theta_2 \\ \vdots \\ \theta_n \end{pmatrix}. \qquad (1)$$

Using Singular Value Decomposition (SVD) [10], the response matrix is

$$R = USV^T, \qquad (2)$$

where $U$ is an $m \times m$ unitary matrix, $V$ is an $n \times n$ unitary matrix, and $S$ is an $m \times n$ rectangular diagonal matrix with eigenvalues $\lambda$ on the diagonal in descending order $\lambda_1 \geq \cdots \geq \lambda_i \geq \lambda_{i+1} \geq \cdots \geq \lambda_{min} \geq 0$. The inverse of the matrix $R$ is

$$R^{-1} = VS^{-1}U^T. \tag{3}$$

The solution to Eq. 1 is

$$\theta = R^{-1} \triangle X. \tag{4}$$

The minimum norm solution which minimizes $\|R\theta - \triangle X\|^2$ is

$$\theta = \sum_{i=1}^{n} \frac{u_i^T \triangle X}{\lambda_i} v_i, \tag{5}$$

where $u$ and $v$ are the vectors of the matrices $U$ and $V$ respectively.

Since small eigenvalues ($\lambda_i$) lead to large corrector currents and since small perturbations in the measured beam positions can lead to large errors if even one eigenvalue is small, truncated SVD [11] may be implemented to avoid this by setting small eigenvalues to zero.

Tikhonov regularization [11, 12], which minimizes $\|R\theta - \triangle X\|^2 + a\|\theta\|^2$, where $a$ is the regularization parameter, may also be used to avoid amplification of errors. Tikhonov regularization is implemented by modifying the eigenvalues using [12]

$$\lambda_i' = \lambda_i + a^2/\lambda_i. \tag{6}$$

With a sufficiently large regularization parameter, the effective weighting of small eigenvalues is increased therefore limiting the required corrector currents. Large eigenvalues are only slightly modified by the regularization, so distortion to the original linear least square problem is minor. The general guidance [12] for initial estimates of the regularization parameter is $\lambda_{max} \gg a \gg \lambda_{min}$.

## 3. Optimization of feedback at fixed energies

The feedback system was first tested in 2010 with 2 correctors and 4 BPMs in each of the two experimental areas [8]. The full feedback system, with 36

BPMs and 12 correctors implemented in 2011 [8], was determined to perform well with only the 24 BPMs near the triplets indicating the absence of additional perturbation sources outside of the regions of the triplets. The eigenvalues for the orbit response matrix at injection energy are shown in Fig. 2. The damping of beam oscillation with feedback at injection energy is shown in Fig. 3 with six small eigenvalues discarded as discussed in the following two subsections. The RMS oscillation amplitude measured at the shown location was reduced from $513\mu m$ to $100\mu m$. The RMS oscillation amplitude averaged over all BPMs was reduced by a factor of $\sim 4$ at injection energy.

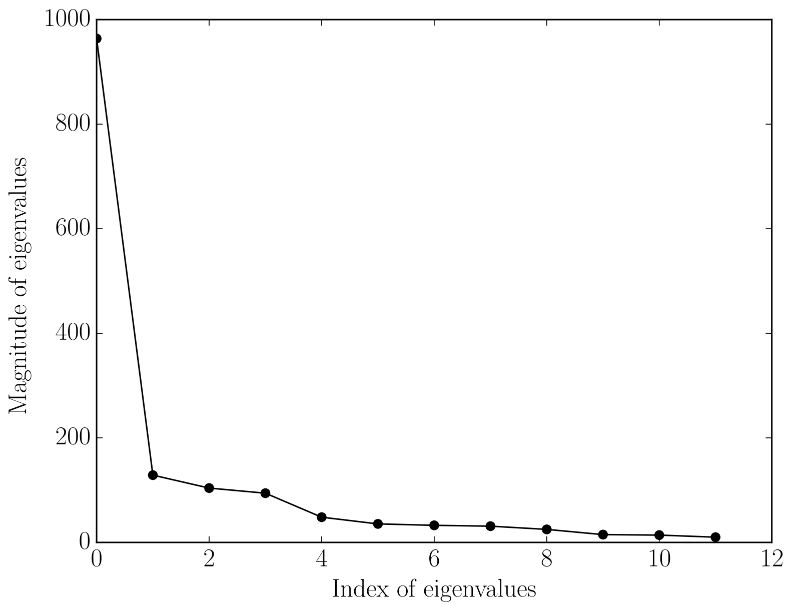


Figure 2: The eigenvalue magnitude versus eigenvalue number for the feedback response matrix at injection energy. The number of eigenvalues is equal to the number of correctors. The eigenvalues are listed in descending order as the diagonal of matrix S (Eq. 2).

In the following two subsections, the simulation approach will be presented followed by experimental observations. It will be shown that the optimal number of eigenvalues to retain obtained in simulation agrees with the experimental results.

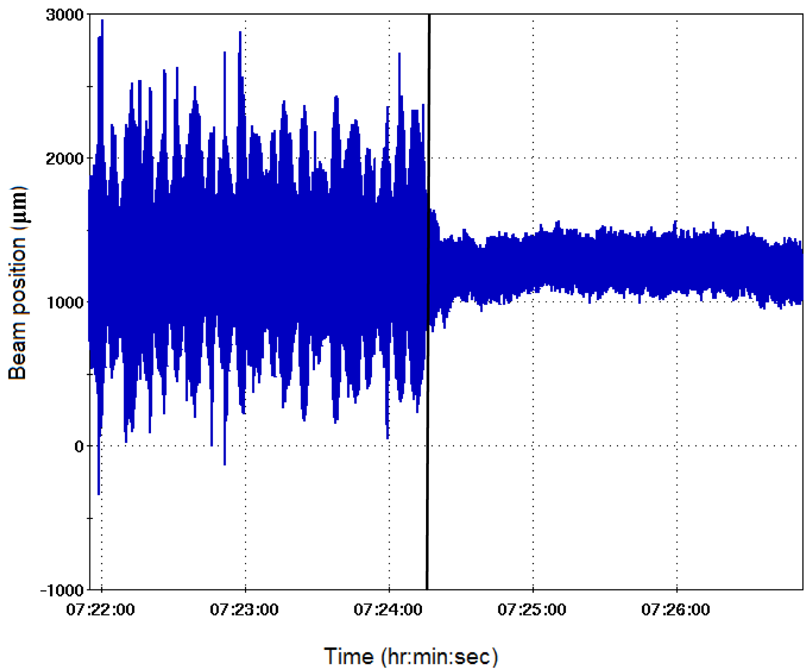


Figure 3: Measured beam position oscillation before and after the 10 Hz global orbit feedback system was engaged at the black vertical line.

### 3.1. Numerical simulation to determine the optimal number of eigenvalues

The optimal number of eigenvalues to retain in the algorithm was determined by simulation including the effect of errors using as input the measured beam positions shown in Fig. 4. The simulated errors included those in the orbit response matrix (ORM, R matrix in Eq. 1) elements and errors in the corrector power supply currents. The relative ORM errors were uniformly distributed in the range of ±20% based on beam-based measurement of the ORM [9]. The errors in corrector currents were uniformly distributed in the range of [-0.03, 0.03]A based on the observed fluctuations in the measured power supply currents.

The simulation was executed as follows. First, the ORM was decomposed using SVD as a function of the number of retained eigenvalues. The required corrector currents were obtained using Eq. 4. The corrector current errors were then added to the derived values and the ORM errors were added to the model ORM. Then the ORM with errors was used together with the corrector currents to calculate the correction of the orbit. The estimated residual orbit is given by the sum of the original orbit and the correction of the orbit. The standard deviation of the residual beam oscillations at the $i$th BPM is

$$\sigma_{x,i} = \sqrt{\sum_{j=1}^{N} (x_{i,j} - < x >_i)^2/(N-1)}, \tag{7}$$

where $N$ is the number of measurements of the beam position, $< x >_i$ is the average position and $x_{i,j}$ is the $j$th sample of the measured beam position at the $i$th BPM. These standard deviations were normalized by the square root of the $\beta$-functions and averaged over $m$ BPMs. The result, $y = \frac{1}{m}\sum_{i=1}^{m} \sigma_{x,i}/\sqrt{\beta_i}$, where $\beta_i$ is the $\beta$-function at the $i$th BPM, is defined as the figure of merit (FOM) of the feedback performance. For each selected number of eigenvalues, 200 simulations were performed with random seeds of errors. The average of the FOMs ($< y >$) is shown along with the average of the maximum corrector currents ($< I_m >$). The error bars show the statistical errors ($\delta y$, $\delta I_m$) from these simulations.

Without errors in the ORM and corrector currents, the dependence of the residual orbit oscillation amplitude and corrector current on the number of retained eigenvalues is shown in Fig. 5. As more eigenvalues are retained, the normalized oscillation amplitude is reduced and larger corrector currents are required to damp beam oscillation.

With errors in the ORM and corrector currents, the simulated residual orbit oscillation amplitude and corrector current are shown in Fig. 6. An optimum of the simulated feedback performance was obtained by retaining 6 eigenvalues.

To investigate the sensitivity of the system's response to errors in the ORM, the feedback performance was also simulated with the relative ORM error in the range of ±90%. The feedback damps beam oscillations in simulation even with

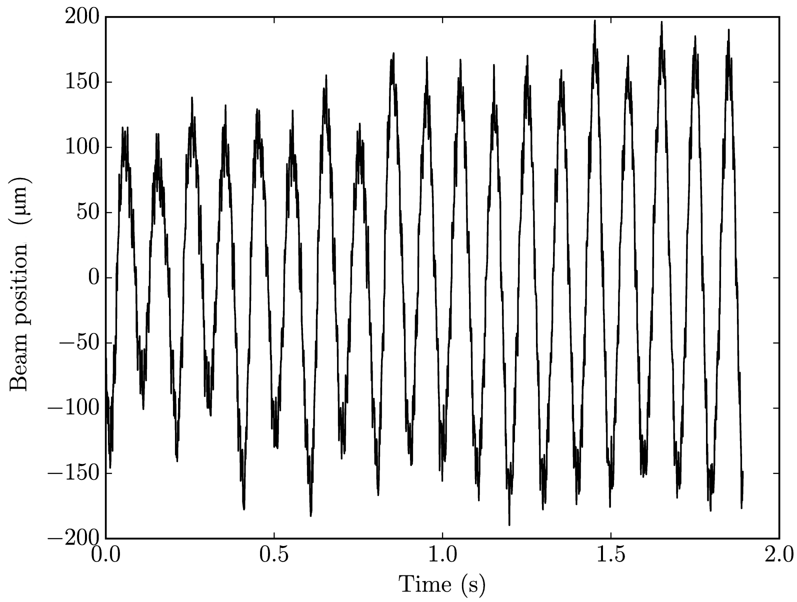


Figure 4: Beam position oscillation measured at a 1 kHz rate over a 2 s time period by one of the BPMs in the feedback system at injection energy with feedback off. Peak-to-peak beam position oscillations at other BPM locations varied between 300 to 3000 $\mu m$ without feedback.

large relative ORM errors. This result is consistent with the fact that the feedback worked as well in the earlier years with peak-to-peak relative $\beta-$function errors on the order of $\sim \pm 80\%$ [13, 14, 15]. The simulations also showed that the larger the relative ORM error, the fewer the number of eigenvalues that should be retained for optimal performance.

Simulations were also performed at top energy. These showed that the optimal performance was achieved when retaining 6 eigenvalues. When retaining 11 or 12 eigenvalues, the simulation also showed that the corrector currents exceeded the upper current limit mainly due to the higher beam rigidity.

### *3.2. Experimental study to determine the optimal number of eigenvalues*

The simulation results were then validated by experiment. The damping of beam oscillations was evaluated as a function of the number of retained

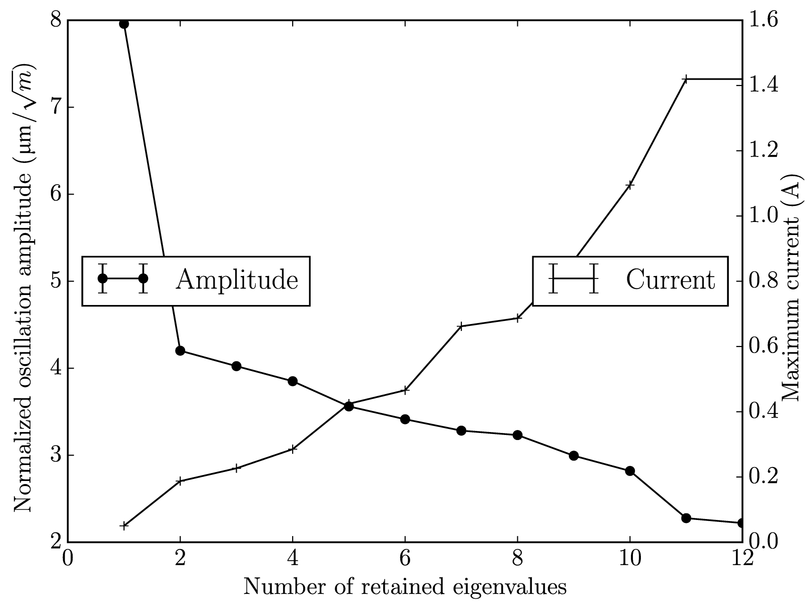


Figure 5: The simulated residual orbit oscillation amplitude and corrector current as a function of the number of retained eigenvalues under ideal conditions with no errors in the orbit response matrix or corrector currents.

eigenvalues. The best performance was confirmed to result when retaining 6 or 7 eigenvalues. The amplitudes of the beam spectrum (the peak amplitude of the Fourier spectrum of beam position measurements acquired at a 1 kHz rate over 2 s) at all BPMs are shown for different number of retained eigenvalues in Fig. 7. The performance for the cases of retaining 6 and 7 eigenvalues is seen to be nearly indiscernible.

## 4. Optimization of feedback during acceleration

At RHIC, the implementation of global orbit feedback during acceleration is complicated by the lowering of the beta functions at the interaction points during acceleration. The $\beta-$functions at the IPs, the beam rigidity and its time-derivative during beam acceleration are shown in Fig. 8 for the 100 GeV polarized proton physics program in 2015. The $\beta-$functions at IP6 and IP8

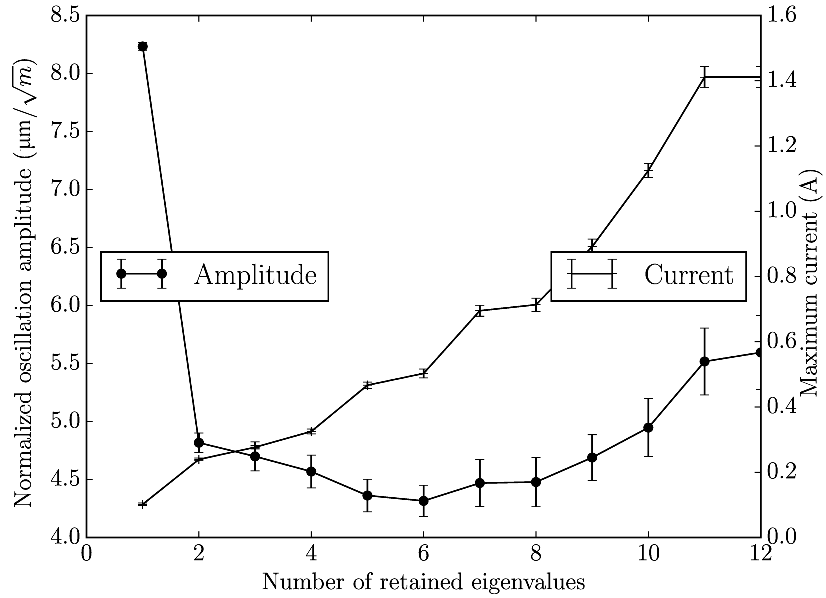


Figure 6: The simulated residual orbit oscillation amplitude and corrector current as a function of the number of retained eigenvalues taking into account errors in the orbit response matrix and corrector currents.

were squeezed from 10 to 2 m, then down to 0.7 m. The $\beta-$functions at other IPs were held constant at 10 m during acceleration.

The configuration of the feedback system during acceleration is different in several aspects with respect to that for fixed energies. Because of the changing beam rigidity, $\sim 200$ response matrices were updated at a 1 Hz rate through the 200 s acceleration cycle. The strength-to-current coefficients for the correctors, which scale with the beam rigidity, were updated at a 1 Hz rate likewise. Since earlier studies at injection and store energies showed that retaining 6 eigenvalues was optimal, the same configuration was applied to all matrices during acceleration. Around transition energy, the global orbit feedback was turned off for 10 seconds.

Shown in Fig. 9 are the recorded beam positions at one BPM both with and without feedback during acceleration [8]. The current of one of the correctors,

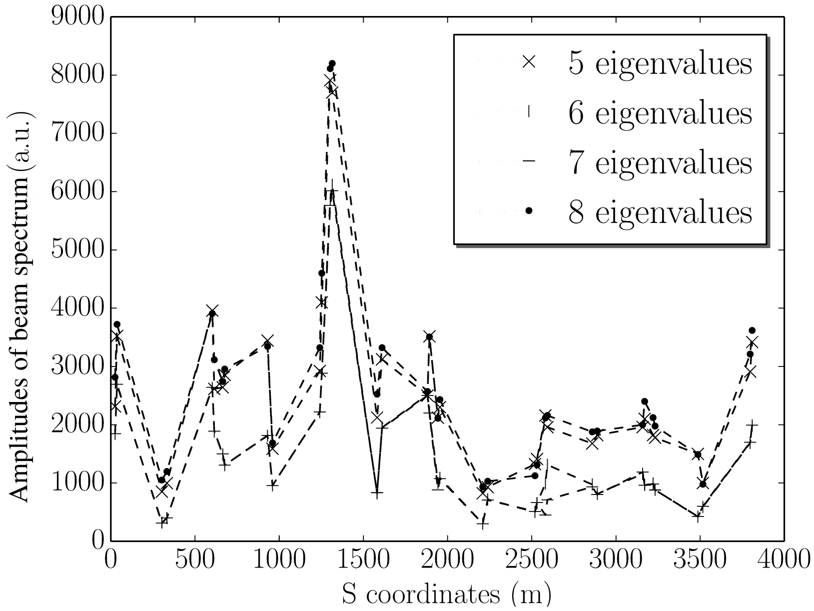


Figure 7: The measured amplitudes of beam spectrum at BPM locations while retaining 5, 6, 7 and 8 eigenvalues.

which increases with beam rigidity during acceleration, is shown in Fig. 10. The amplitudes of the damped beam oscillations and corrector currents are different at different IRs. The damped oscillation amplitudes around IP6 and 8 were measured to be higher than around the other IPs by $\sim$ 50% due to the larger $\beta-$functions at the locations of the beam position monitors. The least-damped oscillation was found around IP10 due to the large distance ($\sim$10 m, 1-2 m at others IPs) between the corrector and the triplet. The corrector current is proportional to $K/\sqrt{\beta}$, assuming the vibration amplitudes of all triplets are equal, where $K$ is the normalized strength of the triplet and $\beta$ is the $\beta-$function at the corrector. Therefore, the currents of the correctors around IP6 and 8 were comparable to those around other IPs with the exception of around IP10. At IP10 higher currents were observed on the correctors around IP10 because the correctors are further away from one of the sources of vibration nearby, the IP10

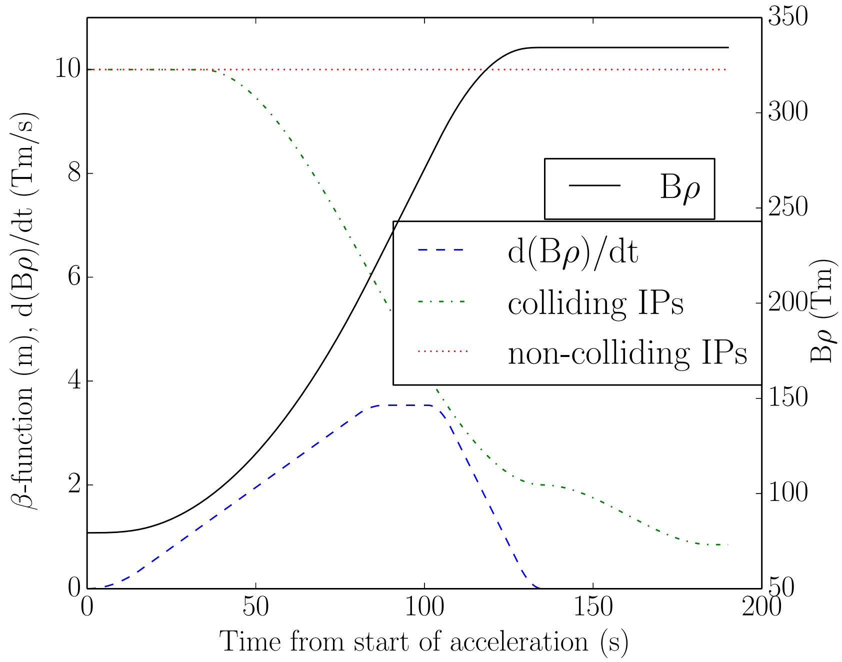


Figure 8: The $\beta$-functions at IPs (red dot, green dash-dot), the beam rigidity $B\rho$ (black solid) and its time-derivative $d(B\rho)/dt$ (blue dash) during acceleration in the 100 GeV polarized proton physics program of 2015. The horizontal axis shows time in seconds from the start of acceleration.

triplets.

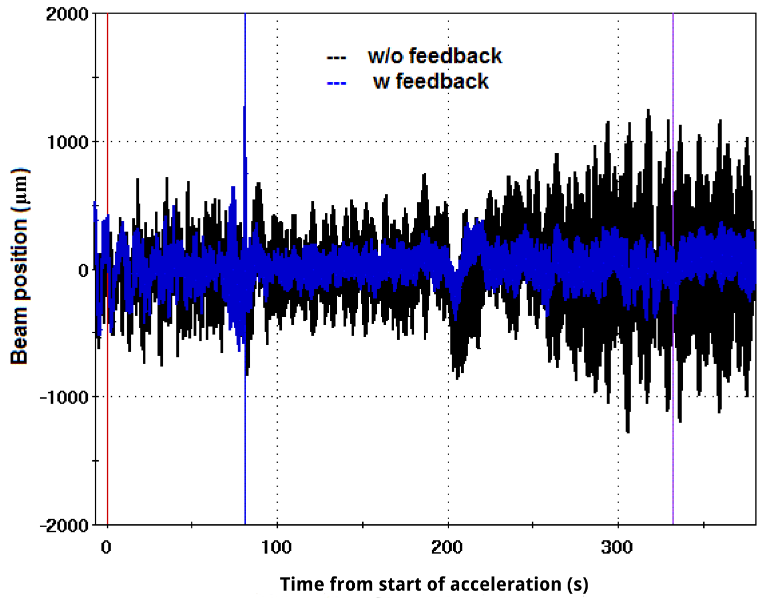


Figure 9: Measured beam position during acceleration with and without feedback. The red vertical line shows the time beam acceleration started, the blue vertical line is at the time when beam cross transition, the magenta line shows when beam acceleration finished.

## 5. Measures to mitigate corrector current transients

While the feedback system successfully damped the beam oscillations during acceleration for years, large amplitude oscillations (upper plot in Fig. 11) and corrector current transients (lower plot in Fig. 11) were observed during acceleration in the polarized proton program of 2015.

### *5.1. Identifying the cause of current transients*

To understand the cause of these current transients during beam acceleration, the eigenvalues were examined first. Due to the changing optics, the eigenvalues vary during acceleration. As shown in Fig. 12, there are sharp peaks of

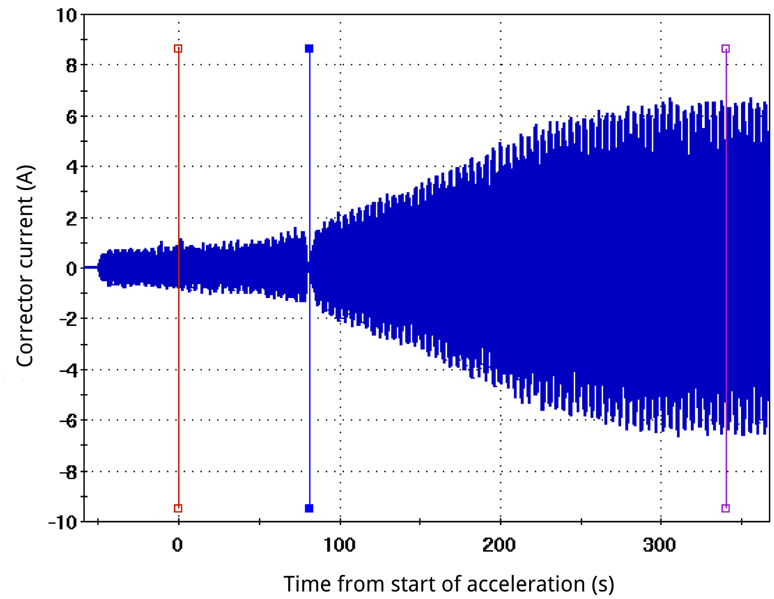


Figure 10: The current of one corrector during beam acceleration with feedback engaged.

the eigenvalues which is the consequence of changes of the orbit response matrix.

The elements of the inverted matrix $R^{-1}$ were examined as well. The first row of the inverted matrix, which consists of 24 matrix elements, was calculated when retaining 6 eigenvalues. The evolution of these matrix elements during acceleration for the polarized proton lattice is shown in Fig. 13. Transients of the corrector currents were observed to be correlated with the step changes of matrix elements during acceleration, which also coincide with the transients of the eigenvalues in Fig. 12. The truncated SVD method [11] can only alleviate the transients to some extent since the method regulates only the selected eigenvalues. Therefore Tikhonov regularization [12], which regulates all eigenvalues and therefore all elements of the inverted matrix, was adopted.

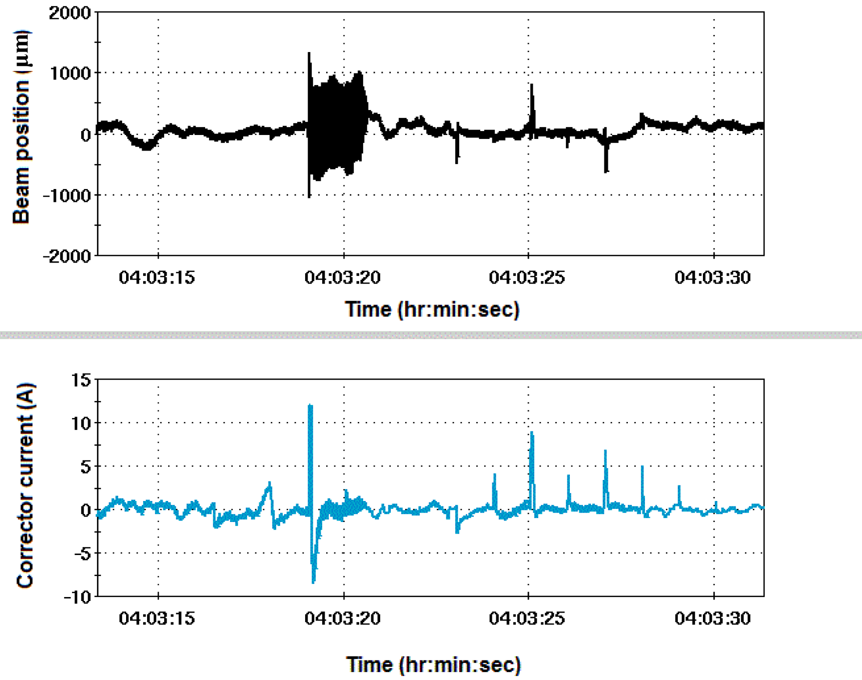


Figure 11: Excitation of beam oscillations (upper plot) and corrector currents (lower plot) during acceleration with polarized proton lattice in 2015 with global orbit feedback engaged.

### *5.2. Matrix smoothing using Tikhonov regularization*

Matrix smoothing using Tikhonov regularization was studied numerically. Tikhonov regularization (Eq. 6) with a constant regularization parameter, $a$, was applied to all matrices during acceleration. Shown in Figs. 14 and 15 are the same group of matrix elements (as in Fig. 13) with $a = 40$ and $a = 100$ respectively. Compared with Fig. 13, the evolution of the matrix elements is observed to be more smooth while the sensitivity to the exact choice of regularization parameter is weak.

### *5.3. Implementation of High-pass filter*

In addition to matrix smoothing using Tikhonov regularization, a digital high-pass filter was introduced to subtract the average measured beam position

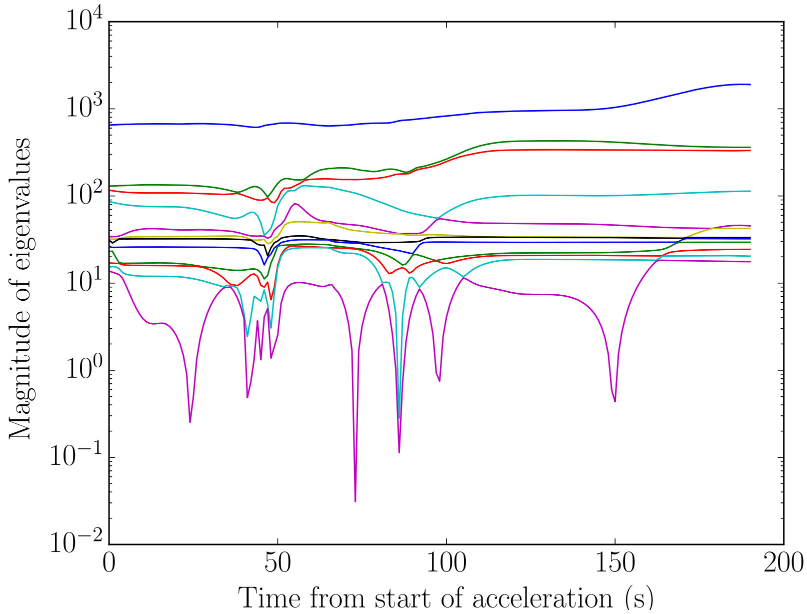


Figure 12: The calculated evolution of the 12 eigenvalues during acceleration for the 100GeV polarized proton program lattice in 2015. The horizontal axis shows the time in seconds from the start of acceleration.

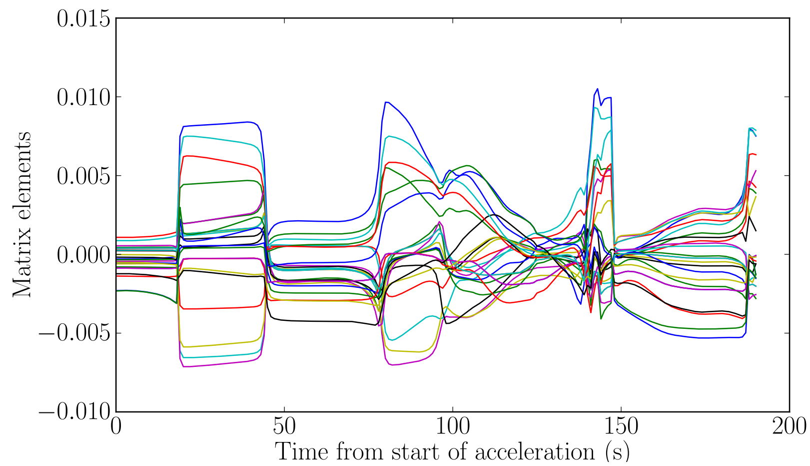


Figure 13: The calculated evolution of selected matrix elements during acceleration with 6 of the 12 eigenvalues retained for the inverted matrix.

at each BPM. With the high-pass filter, the difference between each new beam position value and the running average is corrected. For each corrector, the required correction strength with the high-pass filter is

$$\theta_j = \sum_{i=1}^{m} R_{ji}^{-1} * (< x >_i - x_i), \tag{8}$$

using the same notations as in Eq. 1. Without the high-pass filter, the corrections were calculated without subtracting the average position $< x >_i$. The required correction strength for each corrector without the high-pass filter is

$$\theta_j = \sum_{i=1}^{m} R_{ji}^{-1} * (-x_i). \tag{9}$$

Therefore, the step changes in matrix elements (Fig. 13) were amplified by the average orbit component $< x >_i$ in position measurements $x_i$ in the calculation of corrector currents.

### *5.4. Experimental results*

The corrector current transients during acceleration were eliminated by smoothing the matrix with Tikhonov regularization parameter $a = 100$ and implementation of the high-pass filter. To study the relative contribution of matrix

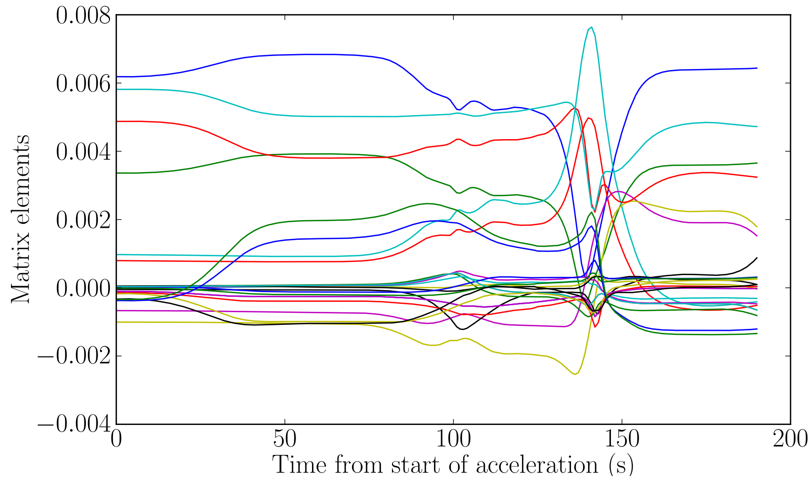


Figure 14: The calculated evolution of selected matrix elements during acceleration with Tikhonov regularization for the inverted matrix with a regularization parameter of 40.

smoothing and the high-pass filter, the matrix smoothing was reverted while maintaining the high-pass filter in a later experiment. The current transients were still observed although less during beam acceleration. Beam studies with only matrix smoothing but without the high-pass filter were not performed due to time constraints. Therefore, it was not determined if matrix smoothing using Tikhonov regularization alone could have eliminated the current transients. A beam study with only matrix smoothing is possible in the future. Meanwhile, simulations to understand the relative contribution of matrix smoothing and the high-pass filter will be performed.

## 6. Summary

In this report, we presented the numerical and experimental optimization of the 10 Hz feedback system and demonstrated that the numerical optimization of feedback performance at fixed beam energies was validated by experimental results. Numerical simulation of orbit feedback with measured beam positions including estimated errors revealed that optimal performance of the feedback

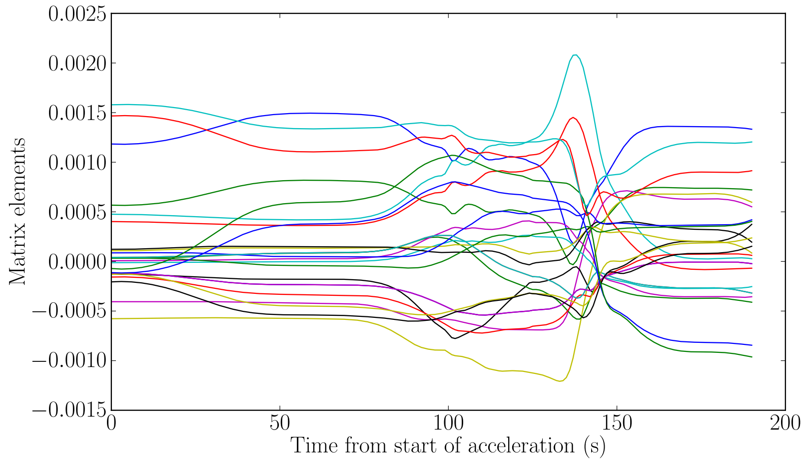


Figure 15: The calculated evolution of selected matrix elements during acceleration with Tikhonov regularization for the inverted matrix with a regularization parameter of 100.

was achieved while retaining 6 eigenvalues in the SVD matrix. The simulation results were confirmed by experimental study. The numerical simulation of orbit feedback, which can be applied for feedback systems at other facilities, was described in this report. The feedback algorithm was first optimized at fixed energies. The configuration for the feedback system during beam acceleration was determined based on the experimentally optimized configurations at injection and top energy.

The corrector current transients encountered during acceleration were eliminated by application of Tikhonov regularization and addition of a high-pass filter. These transients observed with the polarized proton lattice were found to be related to the step changes of the matrix elements and the peaks of eigenvalue evolution during acceleration. Tikhonov regularization was applied to smooth the matrix elements during acceleration. In addition, a digital high-pass filter was implemented to exclude the contributions from static beam offsets. With application of both matrix smoothing and the high-pass filter, the corrector current transients during acceleration were eliminated.

## 7. Acknowledgments

Work supported by Brookhaven Science Associates, LLC under Contract No. DE-AC02-98CH10886 with the U.S. Department of Energy.

## References

[1] M. Harrison, T. Ludlam, and S. Ozaki. RHIC project overview. *Nuclear Instruments and Methods in Physics Research Section A: Accelerators, Spectrometers, Detectors and Associated Equipment*, 499(2):235–244, 2003.

[2] C. Montag, M. Brennan, J. Butler, et al. Measurements of mechanical triplet vibrations in RHIC. *Proceedings of EPAC*, 2002.

[3] C. Montag, R. Bonati, J.M. Brennan, et al. Observation of helium flow induced beam orbit oscillations at RHIC. *Nuclear Instruments and Methods in Physics Research Section A: Accelerators, Spectrometers, Detectors and Associated Equipment*, 564(1):26–31, 2006.

[4] P. Thieberger, R. Bonati, G. Corbin, et al. Recent triplet vibration studies in RHIC. *Proceedings of IPAC*, 2010.

[5] C. Montag, P. He, L. Jia, et al. Helium flow induced orbit jitter at RHIC. *Proceedings of PAC*, 2005.

[6] M. Minty. Effect of triplet magnet vibrations on RHIC performance with high energy protons. *Proceedings of IPAC*, 2010.

[7] C. Montag, A. Marusic, R. Michnoff, et al. Fast IR orbit feedback at RHIC. *Proceedings of PAC*, 2005.

[8] R. Michnoff, L. Arnold, L. Carboni, et al. RHIC 10 Hz global orbit feedback system. *Proceedings of PAC*, 2011.

[9] C. Liu, R. Hulsart, A. Marusic, et al. Near real-time response matrix calibration for 10 Hz GOFB. *Proceedings of IPAC*, 2012.

[10] H. Golub and C. Reinsch. Singular value decomposition and least squares solutions. *Numerische Mathematik*, 14(5):403–420, 1970.

[11] P.C. Hansen. The truncated SVD as a method for regularization. *BIT Numerical Mathematics*, 27(4):534–553, 1987.

[12] A.N. Tikhonov and V.Y. Arsenin. *Solutions of ill-posed problems*. Winston, 1977.

[13] M. Bai, J. Aronson, M. Blaskiewicz, et al. Optics measurements and corrections at RHIC. *Proceedings of IPAC*, 2012.

[14] C. Liu, M. Blaskiewicz, K.A. Drees, et al. Global optics correction in RHIC based on turn-by-turn data from ARTUS tune meter. *Proceedings of NA-PAC*, 2013.

[15] X. Shen, S.Y. Lee, M. Bai, et al. Application of independent component analysis to AC dipole based optics measurement and correction at the Relativistic Heavy Ion Collider. *Physical Review Special Topics-Accelerators and Beams*, 16(11):111001, 2013.